thyX (*24*). As in other strains that lack the most common thymidylate synthase (thyA) but have thyX, HTCC1062 also lacks the dihydrofolate reductase folA (*25*). Evidence suggests that the gene encoding thyX can substitute for folA (*24*). A full glycolytic pathway was not reconstructed because of the confounding diversity of glycolytic pathways (*26*). Five enzymes in the canonical glycolytic pathway were not seen, including two key enzymes involved in allosteric control: phosphofructokinase and pyruvate kinase. An enzyme thought to substitute for pyruvate kinase (*27*), known as PPDK (pyruvate-phosphate dikinase), was found. Some but not all of the enzymes for the nonphosphorylated Entner-Duodoroff pathway, considered more ancient than canonical glycolysis (*26*, *28*), were detected, as well as a complete pathway for gluconeogenesis, also considered more ancient than canonical glycolysis (*29*). Sugar transporters with best BLAST hits to maltose/trehalose transport were found, so presumably a complete glycolytic pathway does function in this cell.

Whole-genome shotgun (WGS) sequence data from the Sargasso Sea segregated at high similarity values, relative to other α-proteobacteria and proteobacteria, in a BLASTN analysis of the *P. ubique* genome (fig. S4). Sequence diversity prevented Venter *et al.* (*19*) from reconstructing SAR11 genomes from the Sargasso Sea WGS data set, although SAR11 rRNA genes accounted for 380 of 1412 16*S* rRNA genes and gene fragments they recovered (26.9%), and the library was estimated to encode the equivalent of about 775 SAR11 genomes. Three Sargasso Sea contiguous sequences (contigs) that were long (5.6 to 22.5 kb) and highly similar to the *P. ubique* genome were analyzed in detail. Genes on these contigs were syntenous with genes from the *P. ubique* genome, with amino acid sequence identities ranging from 68 to 96% (fig. S5). Phylogenetic analysis of four conserved genes from these contigs (those encoding RNA polymerase subunit B, Fig. 3; elongation factor G, fig. S6; DNA gyrase subunit B, fig. S7; and ribosomal protein S12, fig. S8) showed them to be associated with large, diverse environmental clades that branched within the α-proteobacteria. We hypothesize that evolutionary divergence within the SAR11 clade and the accumulation of neutral variation are the most likely explanations for the natural heterogeneity in SAR11 genome sequences.

Metabolic reconstruction failed to resolve why *P. ubique* will not grow on artificial media. When cultured in seawater, it attains cell densities similar to populations in nature, typically 10^5 to 10^6 ml^{-1} depending on the water sample (*3*). No evidence of quorum-sensing systems was found in the genome, and experimental additions of nutrients supported the results from metabolic reconstruction, which suggests that an unusual growth factor may play a role in the ecology of this organism.

P. ubique has taken a tack in evolution that is distinctly different from that of all other heterotrophic marine bacteria for which genome sequences are available. Evolution has divested it of all but the most fundamental cellular systems such that it replicates under limiting nutrient resources as efficiently as possible, with the outcome that it has become the dominant clade in the ocean.

References and Notes

1. R. M. Morris *et al.*, *Nature* **420**, 806 (2002).
2. S. J. Giovannoni *et al.*, *Nature*, in press.
3. M. S. Rappé, S. A. Connon, K. L. Vergin, S. J. Giovannoni, *Nature* **418**, 630 (2002).
4. D. K. Button, *Appl. Environ. Microbiol.* **57**, 2033 (1991).
5. A. Mira, H. Ochman, N. A. Moran, *Trends Genet.* **17**, 589 (2001).
6. M. Kimura, *The Neutral Theory of Molecular Evolution* (Cambridge Univ. Press, Cambridge, 1983).
7. A. Dufresne, L. Garczarek, F. Partensky, *Genome Biol.* **6**, R14 (2005).
8. B. Strehl, J. Holtzendorff, F. Partensky, W. R. Hess, *FEMS Microbiol. Lett.* **181**, 261 (1999).
9. G. Rocap *et al.*, *Nature* **424**, 1042 (2003).
10. D. W. Ussery, P. F. Hallin, *Microbiology* **150**, 749 (2004).
11. D. A. Hansell, C. A. Carlson, *Global Biogeochem. Cycles* **12**, 443 (1998).
12. D. A. Hansell, C. A. Carlson, *Deep Sea Res.* **48**, 1649 (2001).
13. R. R. Malmstrom, R. P. Kiene, M. T. Cottrell, D. L. Kirchman, *Appl. Environ. Microbiol.* **70**, 4129 (2004).
14. D. K. Button, B. Robertson, E. Gustafson, X. Zhao, *Appl. Environ. Microbiol.* **70**, 5511 (2004).
15. S. G. Andersson *et al.*, *Nature* **396**, 133 (1998).
16. S. Elsen, L. R. Swem, D. L. Swem, C. E. Bauer, *Microbiol. Mol. Biol. Rev.* **68**, 263 (2004).
17. E. G. Ruby *et al.*, *Proc. Natl. Acad. Sci. U.S.A.* **102**, 3004 (2005).
18. B. D. Lanoil, L. M. Ciufettii, S. J. Giovannoni, *Genome Res.* **6**, 1160 (1996).
19. J. C. Venter *et al.*, *Science* **304**, 66 (2004); published online 4 March 2004 (10.1126/science.1093857).
20. M. A. Moran *et al.*, *Nature* **432**, 910 (2004).
21. C. A. Carlson, H. W. Ducklow, A. F. Michaels, *Nature* **371**, 405 (1994).
22. F. Azam, *Science* **280**, 694 (1998).
23. J. A. Klappenbach, J. M. Dunbar, T. M. Schmidt, *Appl. Environ. Microbiol.* **66**, 1328 (2000).
24. H. Myllykallio *et al.*, *Science* **297**, 105 (2002); published online 23 May 2002 (10.1126/science.1072113).
25. H. Myllykallio, D. Leduc, J. Filee, U. Liebl, *Trends Microbiol.* **11**, 220 (2003).
26. T. Dandekar, S. Schuster, B. Snel, M. Huynen, P. Bork, *Biochem. J.* **343**, 115 (1999).
27. R. E. Reeves, R. A. Menzies, D. S. Hsu, *J. Biol. Chem.* **243**, 5486 (1968).
28. E. Melendez-Hevia, T. G. Waddell, R. Heinrich, F. Montero, *Eur. J. Biochem.* **244**, 527 (1997).
29. R. S. Ronimus, H. W. Morgan, *Archaea* **1**, 199 (2003).

30. Supported by NSF grant EF0307223, Diversa Corporation, the Gordon and Betty Moore Foundation, and the Oregon State University Center for Gene Research and Biotechnology. We thank S. Wells, M. Hudson, D. Barofsky, M. Staples, J. Garcia, B. Buchner, P. Sammon, K. Li, and J. Ritter for technical assistance and J. Heidelberg for advice about genome assembly. We also acknowledge the crew of the R/V Elakha for assistance with sample and seawater collections, the staff of the Central Services Laboratory at Oregon State University for supplementary sequence analyses, and the staff of the Mass Spectrometry Laboratory at Oregon State University for proteomic analyses. The sequence reported in this study has been deposited in GenBank under accession number CP000084.

Supporting Online Material

www.sciencemag.org/cgi/content/full/309/5738/1242/DC1
Materials and Methods
Tables S1 to S3
Figs. S1 to S9
References

26 April 2005; accepted 11 July 2005
10.1126/science.1114057

Contact-Dependent Inhibition of Growth in *Escherichia coli*

Stephanie K. Aoki, Rupinderjit Pamma, Aaron D. Hernday, Jessica E. Bickham, Bruce A. Braaten, David A. Low*

Bacteria have developed mechanisms to communicate and compete with each other for limited environmental resources. We found that certain *Escherichia coli*, including uropathogenic strains, contained a bacterial growth-inhibition system that uses direct cell-to-cell contact. Inhibition was conditional, dependent upon the growth state of the inhibitory cell and the pili expression state of the target cell. Both a large cell-surface protein designated Contact-*d*ependent *i*nhibitor A (CdiA) and two-partner secretion family member CdiB were required for growth inhibition. The CdiAB system may function to regulate the growth of specific cells within a differentiated bacterial population.

Bacteria communicate with each other in multiple ways, including the secretion of signaling molecules that enable a cell population to determine when it has reached a certain density or that a potential partner is present for conjugation (*1*, *2*). Cellular communication can also occur through contact between cells, as has been shown for *Myxococcus xanthus*, which undergoes a complex developmental pathway (*3*, *4*). Here we describe a different type of intercellular interaction in which bacterial growth is regulated by direct cell-to-cell contact.

Wild-type *Escherichia coli* isolate EC93 inhibited the growth of laboratory *E. coli* K-12

Molecular, Cellular, and Developmental Biology, University of California–Santa Barbara (UCSB), Santa Barbara, CA 93106, USA.

*To whom correspondence should be addressed. E-mail: low@lifesci.ucsb.edu

strains, such as MG1655, when the bacteria were mixed together in shaking liquid culture (Fig. 1A). In contrast, *E. coli* K-12 strains in general (e.g., EPI100) did not express growth-inhibitory activity (Fig. 1A). We isolated genes from strain EC93, *cdiA* and *cdiB*, that when expressed in *E. coli* K-12 conferred a growth-inhibitory phenotype (Fig. 1A). Growth inhibition was dependent upon the growth state of the inhibitory cells, occurring in logarithmic but not stationary phase. Target cells, however, were inhibited regardless of their growth phase (fig. S1). Protein synthesis also appeared to be required for inhibition, because *cdiA*$^+$*B*$^+$ *E. coli* inhibitor cells pretreated for 2 hours with chloramphenicol did not have measurable inhibitory activity (fig. S2). Experiments measuring the inhibitor-to-target ratio over time (fig. S3) indicate that one *cdiA*$^+$*B*$^+$ *E. coli* cell inhibited the growth of multiple target cells. Starting at an initial ratio of 1 inhibitor to 10 target cells, after 1 hour this ratio increased more than a thousandfold (fig. S3). In contrast, a control experiment with *cdiAB*-negative cells in place of *cdiA*$^+$*B*$^+$ inhibitory cells showed that the control-to-target ratio was not altered over the 3-hour time course (fig. S3).

The growth-inhibitory activity did not appear to be a colicin, which is a secreted antimicrobial peptide, because supernatant solutions from logarithmic phase EC93 cultures lacked inhibitory activity even when a known inducer of colicin synthesis, mitomycin C, was present (*5*, *6*). To test the possibility that induction of inhibitory activity might occur only when target cells are present, we prepared conditioned medium from a mixed culture of *cdiA*$^+$*B*$^+$ inhibitor cells and *E. coli* K-12 target cells (with a 10:1 inhibitor-to-

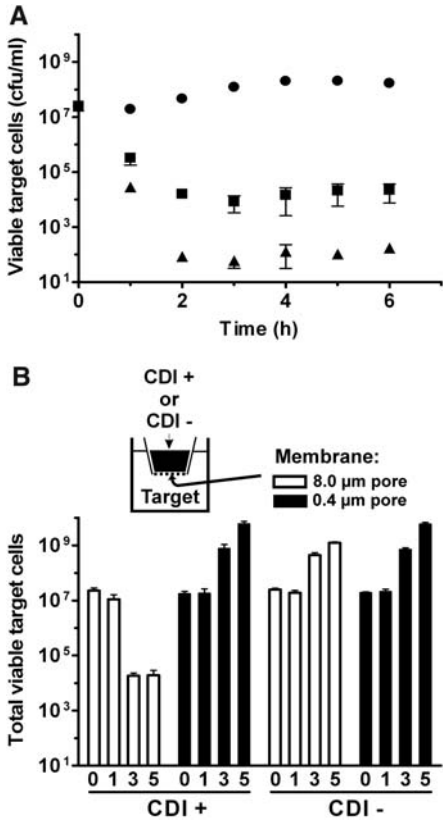

Fig. 1. Contact-dependent inhibition of bacterial growth. (**A**) Target *E. coli* MG1655 tet^R cells were mixed with the following test strains: *E. coli* EC93 inhibitory cells (squares); *E. coli* K-12 EPI100 str^R containing pDAL660Δ1-39 (*cdiA*$^+$*B*$^+$, triangles); and control *E. coli* K-12 EPI100 str^R (circles). The inhibitor-to-target ratio for these experiments was 10:1. At the times indicated, viable target cell counts were obtained. CFU, colony-forming units. (**B**) *E. coli* CDI$^+$ K-12 (DL4577) or CDI$^-$ *E. coli* K-12 (DL4527) were grown to logarithmic phase and added to the top chamber of a six-well plate containing either a 0.4-μm (solid bars) or an 8-μm (open bars) PET membrane. Target *E. coli* MG1655 tet^R cells were added to the bottom well (in a 20:1 inhibitor-to-target ratio). Viable counts for the top and bottom chambers were measured after incubation (hours). Data are means ± SEM; $n = 2$.

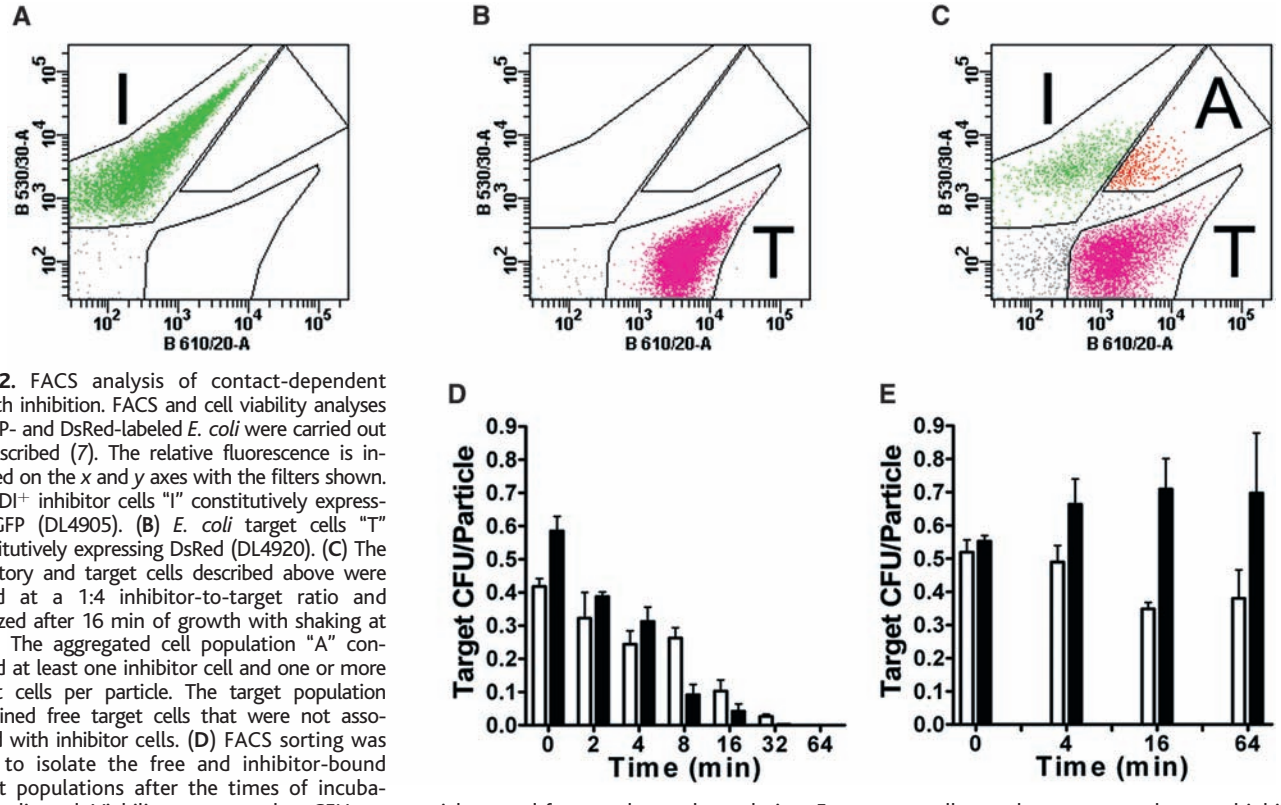

Fig. 2. FACS analysis of contact-dependent growth inhibition. FACS and cell viability analyses of GFP- and DsRed-labeled *E. coli* were carried out as described (*7*). The relative fluorescence is indicated on the *x* and *y* axes with the filters shown. (**A**) CDI$^+$ inhibitor cells "I" constitutively expressing GFP (DL4905). (**B**) *E. coli* target cells "T" constitutively expressing DsRed (DL4920). (**C**) The inhibitory and target cells described above were mixed at a 1:4 inhibitor-to-target ratio and analyzed after 16 min of growth with shaking at 37°C. The aggregated cell population "A" contained at least one inhibitor cell and one or more target cells per particle. The target population contained free target cells that were not associated with inhibitor cells. (**D**) FACS sorting was used to isolate the free and inhibitor-bound target populations after the times of incubation indicated. Viability was scored as CFUs per particle sorted from each gated population. Free target cells are shown as open bars, and inhibitor-bound target cells are shown as solid bars. (**E**) As in (D), except that CDI$^-$ *E. coli* containing *cdiA-FLAG1* (DL4955) was mixed with target cells (DL4920).

target ratio). Target cell viability was reduced more than a thousandfold after 1 hour of incubation (fig. S4A), indicating substantial growth inhibitory activity. Conditioned medium from this 1-hour mixture, when added to fresh K-12 target cells, did not affect cell growth compared to conditioned medium from control *cdiA*$^{-}$*B*$^{-}$ cell mixtures (fig. S4B).

We tested the possibility that growth inhibition might occur through cell-to-cell contact by separating *cdiA*$^{+}$*B*$^{+}$ inhibitory cells from target cells, using polyethylene terephthalate (PET) porous membranes in a six-well plate (Fig. 1B). Growth inhibition was not observed when contact between inhibitory cells and target cells was blocked by 0.4-μm pores; however, growth inhibition (~1000-fold) was observed when 8-μm pores were used, allowing inhibitor and target cell mixing. Addition of *cdiAB*-negative control *E. coli* did not affect growth of target cells, regardless of pore size (Fig. 1B). We obtained similar results using EC93, from which the *cdiAB* genes were isolated for cloning into *E. coli* K-12 (*5*). A potential caveat is that a secreted inhibitory molecule might bind to the PET membrane and be sequestered or inactivated. However, addition of excess PET membranes did not affect the ability of *cdiA*$^{+}$*B*$^{+}$ *E. coli* K-12 to inhibit cell growth (fig. S5). Similar results were obtained with polycarbonate membranes (*5*). These results support the hypothesis that growth inhibition mediated by *cdiAB* requires cell-to-cell contact, designated as contact-dependent inhibition (CDI).

It is possible that the inhibitory factor could be an unstable secreted molecule that is only effectively delivered to target cells in close proximity. To address this possibility, we mixed fluorescently labeled *cdiA*$^{+}$*B*$^{+}$ inhibitory cells [green fluorescent protein (GFP)–labeled] with *E. coli* K-12 target cells [Discosoma red (DsRed)–labeled], and after incubation with shaking, the cell mixtures were sorted by fluorescence-activated cell sorting (FACS). We observed three cell populations, corresponding to green inhibitory cells, red target cells, and cell aggregates containing at least one inhibitory and one target cell per aggregate particle (Fig. 2, A to C). The appearance of the aggregated particles was dependent upon *cdiAB,* indicating that CdiAB mediates intercellular binding (*5*). If cell-to-cell contact were required for growth inhibition, then the viability of target cells bound to inhibitory cells should decrease more rapidly than the viability of free target cells (Fig. 2D). The viability of aggregated targets compared with free targets decreased at time points of 8 min and longer, indicating that observable growth inhibition occurred after 4 to 8 min of contact. Although the viability of free targets was only marginally reduced at times up to 8 min, at later times viability was significantly reduced, albeit at a lesser rate than for aggregated targets (Fig. 2D). It is likely that the observed reduction in viability of "free" target cells was primarily the result of prior contact with *cdiA*$^{+}$*B*$^{+}$ inhibitory cells and release from cell aggregates.

The rapid decrease in viability of the aggregated targets might be due to a nonspecific effect of intercellular binding. FACS analysis was carried out using a *cdiA* mutant (Fig. 3A, *cdiA-FLAG1*) that no longer conferred CDI but retained intercellular adhesion. Under these conditions, the viability of aggregated target cells was not reduced compared to free target cells over the same time course (Fig. 2E), showing that the rapid decrease in viability of target cells bound to inhibitory cells required CDI activity. These results strongly indicate that CdiAB mediates growth inhibition through cell-to-cell contact.

We cloned a DNA region from *E. coli* EC93 that conferred a CDI^{+} phenotype to *E. coli* K-12 and generated 15 base-pair (bp) insertions within the region (*7*). Stop codon insertions within open reading frames (ORFs) designated *cdiA* and *cdiB* (GenBank accession no. DQ100454) abolished CDI activity (Fig. 3A), showing that the *cdiA* and *cdiB* ORFs were necessary for CDI. In addition, we identified a small ORF (Fig. 3A, *cdiI*) adjacent to *cdiA* that conferred full immunity to CDI (fig. S6), explaining why cells expressing *cdiAB* do not inhibit their own growth. The translated *cdiA* and *cdiB* ORFs showed significant amino acid sequence identity with two-partner secretion proteins (fig. S7) that are proteolytically processed during export to the cell surface (*8*). Using FLAG epitope tagging (Fig. 3A), we found that CdiA was expressed as a 303-kD protein on the cell surface (*5*), which was then processed to 284-kD and 195-kD proteins (Fig. 3B). A FLAG insertion in the *cdiB* ORF yielded a 56-kD protein, consistent with the predicted

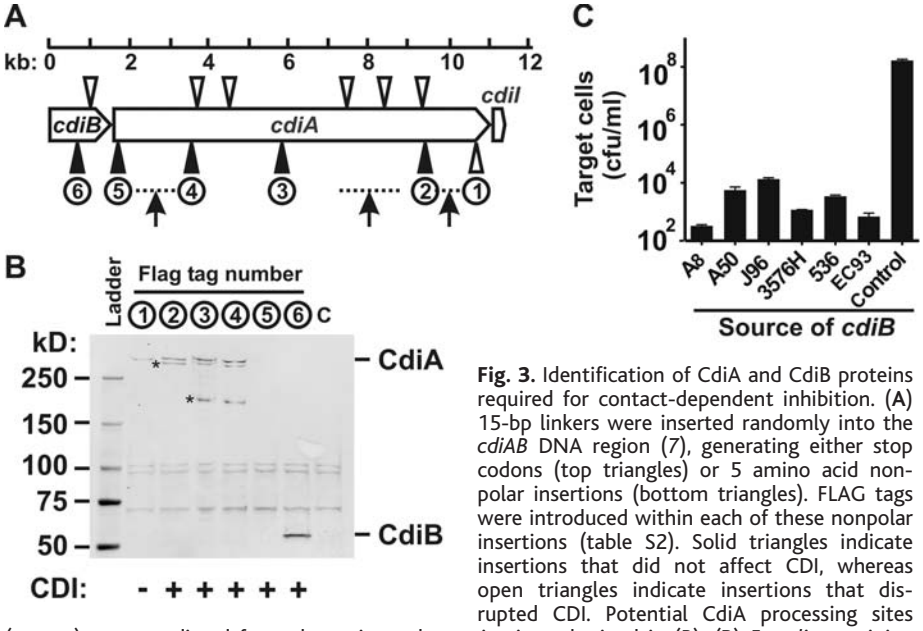

Fig. 3. Identification of CdiA and CdiB proteins required for contact-dependent inhibition. (**A**) 15-bp linkers were inserted randomly into the *cdiAB* DNA region (*7*), generating either stop codons (top triangles) or 5 amino acid nonpolar insertions (bottom triangles). FLAG tags were introduced within each of these nonpolar insertions (table S2). Solid triangles indicate insertions that did not affect CDI, whereas open triangles indicate insertions that disrupted CDI. Potential CdiA processing sites (arrows) were predicted from the estimated protein sizes obtained in (B). (**B**) *E. coli* containing CdiA and B proteins labeled with FLAG tags (lanes 1 to 6) or no FLAG tag control (lane C) were analyzed by SDS–polyacrylamide gel electrophoresis and immunoblotting with monoclonal antiserum to FLAG. A molecular weight ladder and CdiA and CdiB protein positions are shown. Asterisks indicate CdiA fragments, and CDI phenotypes are shown at the bottom. (**C**) *cdiB* homologs from five UPEC isolates and *cdiB* from EC93 were cloned in plasmid pCC1 and tested for CDI complementation in *cdiA*$^{+}$*B*$^{-}$ *E. coli* (DL4958). Vector control plasmid pCC1 is shown (control).

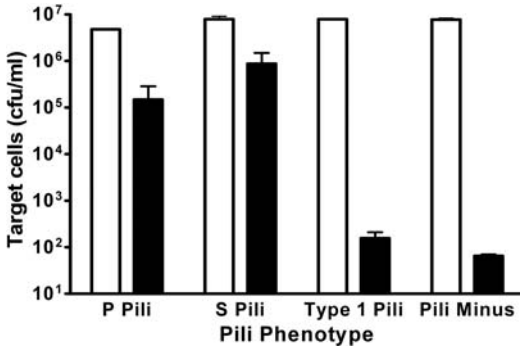

Fig. 4. Effect of Pap pili expression on CDI. *E. coli* HB101 rif^{R} target cells lacking pili (*18*) were transformed with plasmids expressing P pili, S pili, type 1 pili, or plasmid vector alone (pili minus) as indicated at the bottom. Target cells were incubated with CDI^{+} inhibitory *E. coli* DL4577. Viable target cell counts at 0 and 3 hours are depicted by open and solid bars, respectively.

size of CdiB. Proteolytic fragments of CdiA were detected in the growth medium (*5*) but were not growth-inhibitory (fig. S4), indicating that the secreted forms of CdiA are inactive.

High amino acid sequence identity was found between CdiA/CdiB and predicted proteins from uropathogenic *E. coli* (UPEC), including strain 536 (*9*). Complementation analysis indicated that UPEC 536 and four additional UPEC strains contain genes that are functional homologs of *cdiB* (Fig. 3C) and *cdiA* (fig. S8). Bioinformatic analysis showed that *Yersinia pestis* (plague) and *Burkholderia pseudomallei* (melioidosis) also encode possible CdiAB homologs (fig. S7). Filamentous hemagglutinin from *Bordetella pertussis* (whooping cough) appeared more distantly related, sharing sequence identity to CdiA primarily in the N-terminal portion of the protein (fig. S7).

The *cdiAB* homologs in UPEC 536 are present within pathogenicity island II (*10*), but a *cdiI* homolog is not present, nor is it found in the sequenced genome of UPEC CFT073, which also contains a *cdiAB* homolog (*11*). This observation suggests that *cdiAB* expression in UPEC strains would inhibit their growth. Pathogenicity island II in UPEC 536 also contains a pyelonephritis-associated pili (*pap*) operon closely linked to *cdiAB*. Because Pap pili are expressed at the cell surface, we tested the possibility that pili expression might affect CDI because contact between CdiA and the target cell surface could be blocked. *E. coli* K-12 constitutively expressing P pili (*12*) or S pili (*13*) showed resistance to CDI, whereas cells expressing type 1 pili were 1000- to 10,000-fold more sensitive to growth inhibition (Fig. 4). Thus, resistance to CDI conferred by P and S pili involves specific interaction(s) and is not likely to be the result of nonspecific steric hindrance that blocks cell-to-cell contact.

Many UPEC strains contain *fim* (type 1 pili), *pap* (P pili), and *sfa* (S pili) operons (*10*, *11*). The expression of these pili types is normally subject to reversible off/on switching, generating diversity within bacterial populations by a differentiation mechanism (*14*, *15*). Such a mechanism might play a role in the temporal control of the differentiation observed for UPEC strains inside bladder cells, during which the bacteria progress through distinct developmental stages, including a quiescent growth state (*16*). *E. coli* K-12 cells inhibited by CDI appear to be nonviable because of their lack of growth on agar medium. However, CDI-inhibited cells appeared to be viable because they excluded propidium iodide (*5*), a standard criterion for distinguishing viable cells from nonviable cells (*17*). The identification of this sophisticated mechanism in *E. coli,* with possible homologs in a broad range of species, opens the door for exploration of the potential roles of CDI in controlling bacterial development and pathogenesis.

References and Notes

1. J. M. Henke, B. L. Bassler, *Trends Cell Biol.* **14**, 648 (2004).
2. G. J. Lyon, R. P. Novick, *Peptides* **25**, 1389 (2004).
3. R. Welch, D. Kaiser, *Proc. Natl. Acad. Sci. U.S.A.* **98**, 14907 (2001).
4. L. Jelsbak, L. Sogaard-Andersen, *Curr. Opin. Microbiol.* **3**, 637 (2000).
5. S. K. Aoki, A. D. Hernday, R. Pamma, B. A. Braaten, D. A. Low, unpublished data.
6. R. Spangler, S. P. Zhang, J. Krueger, G. Zubay, *J. Bacteriol.* **163**, 167 (1985).
7. Materials and methods are available as supporting material on *Science* Online.
8. G. Renauld-Mongenie, J. Cornette, N. Mielcarek, F. D. Menozzi, C. Locht, *J. Bacteriol.* **178**, 1053 (1996).
9. S. Knapp, J. Hacker, T. Jarchau, W. Goebel, *J. Bacteriol.* **168**, 22 (1986).
10. U. Dobrindt *et al.*, *Infect. Immun.* **70**, 6365 (2002).
11. R. A. Welch *et al.*, *Proc. Natl. Acad. Sci. U.S.A.* **99**, 17020 (2002).
12. D. Low, E. N. Robinson Jr., Z. A. McGee, S. Falkow, *Mol. Microbiol.* **1**, 335 (1987).
13. T. Schmoll *et al.*, *Microb. Pathog.* **9**, 331 (1990).
14. I. C. Blomfield, *Adv. Microb. Physiol.* **45**, 1 (2001).
15. A. D. Hernday, B. A. Braaten, D. A. Low, *Mol. Cell* **12**, 947 (2003).
16. S. S. Justice *et al.*, *Proc. Natl. Acad. Sci. U.S.A.* **101**, 1333 (2004).
17. L. Boulos, M. Prevost, B. Barbeau, J. Coallier, R. Desjardins, *J. Microbiol. Methods* **37**, 77 (1999).
18. I. Johanson, R. Lindstedt, C. Svanborg, *Infect. Immun.* **60**, 3416 (1992).

19. We thank P. Cotter and S. Poole for helpful discussion, J. Hacker for *E. coli* UPEC 536, M. Mulvey for antisera to Type 1 pili, and K. Dane and P. Daugherty (UCSB) for FACS technical assistance. Supported by a Cottage Hospital Research Grant (UCSB), a University of California Biotechnology grant (no. 2002-14), and NIH grant no. AI23348 (D.A.L.).

Supporting Online Material

www.sciencemag.org/cgi/content/full/309/5738/1245/DC1
Materials and Methods
Figs. S1 to S8
Tables S1 and S2

20 May 2005; accepted 11 July 2005
10.1126/science.1115109

Genome-Wide RNAi Screen for Host Factors Required for Intracellular Bacterial Infection

Hervé Agaisse,[1,2]*†‡ Laura S. Burrack,[1]* Jennifer A. Philips,[2] Eric J. Rubin,[3] Norbert Perrimon,[2] Darren E. Higgins[1]‡

Most studies of host-pathogen interactions have focused on pathogen-specific virulence determinants. Here, we report a genome-wide RNA interference screen to identify host factors required for intracellular bacterial pathogenesis. Using *Drosophila* cells and the cytosolic pathogen *Listeria monocytogenes*, we identified 305 double-stranded RNAs targeting a wide range of cellular functions that altered *L. monocytogenes* infection. Comparison to a similar screen with *Mycobacterium fortuitum*, a vacuolar pathogen, identified host factors that may play a general role in intracellular pathogenesis and factors that specifically affect access to the cytosol by *L. monocytogenes*.

During bacterial infections, macrophages play a critical role in eliminating engulfed pathogens. However, intracellular bacterial pathogens have evolved varying strategies to avoid elimination by host macrophages (*1*). One strategy used by pathogens, such as *Mycobacterium tuberculosis*, is to modify the phagosomal compartment to allow for vacuolar replication (*2*). Other bacterial pathogens, such as *Listeria monocytogenes*, escape the phagocytic vacuole to enter the host cell cytosol where replication occurs (*3*). Whereas numerous bacterial determinants that facilitate intracellular infection have been characterized from diverse bacterial species (*4*), less is known about the host factors that are exploited or subverted by intracellular bacterial pathogens. Here, we report the results of a genome-wide RNA interference (RNAi) screen conducted in *Drosophila* SL2 cells to identify host factors required for infection by *L. monocytogenes*, a cytosolic pathogen. In addition, we present the results of a comparison to a similar RNAi screen conducted with *Mycobacterium fortuitum*, a vacuolar pathogen (*5*).

Both *Drosophila* and cultured *Drosophila* cells are tractable models for analysis of *L. monocytogenes* pathogenesis (*6*, *7*). We tested the ability of macrophage-like *Drosophila* SL2 cells to support intracellular infection by *L. monocytogenes*. DH-L1039, a green fluorescent protein (GFP)–expressing *L. monocytogenes* strain derived from wild-type 10403S, replicated within *Drosophila* SL2 cells (fig. S1, A and B). In contrast, GFP fluorescence of DH-L1137, a variant lacking the pore-forming cytolysin listeriolysin O (LLO), was punctate in appearance and growth was inefficient in SL2 cells (fig. S1, A and B), consistent with LLO-negative bacteria that remained trapped within phagocytic vacuoles (*3*, *8*). Next, we developed a microscopy-based, high-throughput RNAi screen to identify host factors required for intracellular infection by *L. monocytogenes* (Fig.

Contact-Dependent Inhibition of Growth in *Escherichia coli*

Stephanie K. Aoki, Rupinderjit Pamma, Aaron D. Hernday, Jessica E. Bickham, Bruce A. Braaten and David A. Low

Science **309** (5738), 1245-1248.
DOI: 10.1126/science.1115109